

section III presents the active and reactive control of DFIG in WECS. Conventional and direct current vector control of GSC is presented in section IV. In section V presents the real and reactive power control of RSC. Then, the fuzzy logic controller presented in section VI. Simulation studies are conducted in section VII to compare the performance of DFIG wind turbine using the direct vector and traditional vector control configuration for steady and variable wind conditions. Finally, this paper concluded with the summary of main points.

2. DFIG mechanical system and power flow operation

A. DFIG mechanical system

A DFIG wind turbine primarily consists of three parts: a wind turbine drive train, an induction generator and power electronic converter (Fig. 2) [2], [4]. In the wind turbine drive train, the blades of the rotor turbine catch wind energy that is then transferred to the induction generator via gearbox. The induction generator is a standard wound rotor induction machine with its stator windings directly connected to the grid and its rotor winding connected to the grid through a voltage source converter. The voltage source converter is built by two self-commutated voltage source converters, the RSC and the GSC with intermediate dc voltage link.

B. Power flow in DFIG

The DFIG can be operated in two modes of operation namely; sub-synchronous and super-synchronous mode depending on the rotor speed below and above the synchronous speed. Figure.2 shows the basic scheme adopted in the majority of systems. The stator winding is directly connected to the AC mains, whilst the rotor winding is fed from the Power Electronics Converter via slip rings to allow DIFG to operate at different speeds in response to changing the wind speed. Indeed, the basic concept is to interpose a frequency converter between the variable frequency induction generator and fixed frequency grid. The DC capacitor linking [5] stator- side and rotor-side converters allows the storage of power from induction generator for further power generation. To achieve full control of grid current and DC-link voltage.

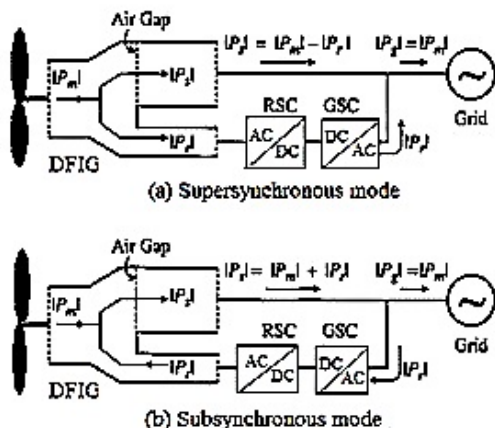


Fig. 3. Power flow in DFIG wind energy conversion system

The slip power can flow in both directions grid to rotor as well as rotor to grid in, i.e. to the rotor from the supply and from supply to the rotor and hence the speed of the machine can be controlled from either rotor-side or stator-side converter in both above and below-synchronous speed ranges. The wound rotor induction machine can be controlled as a generator at or a motor in both super and sub-synchronous operating modes. [6] The sub synchronous speed in the motoring mode and super synchronous speed in the generating mode, RSC operates as a rectifier and GSC as an inverter at that time the slip power is returned to the stator. RSC operates as an inverter and GSC as a rectifier at that time where slip power is supplied to the rotor winding. At the synchronous speed, slip power is taken from supply to excite the rotor windings and in this case machine behaves as a synchronous machine.

3. Active and reactive power control of DFIG

The per phase equivalent for a DFIG is shown in the figure 4. Variables with the ' notation denote rotor quantities as seen from stator side. By neglecting the effects of R_s , jX_{ls} and jX_{lr} the per phase stator power S_s and rotor power S_r Can be expressed as,

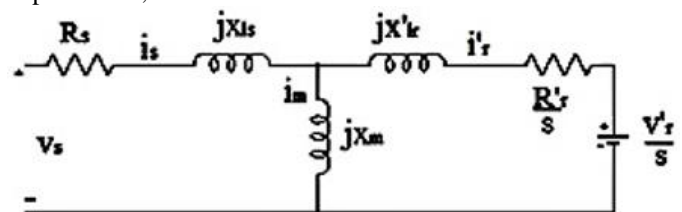


Fig. 4. Per Phase Equivalent Circuit of a DFIG

$$S_s = P_s + jQ_s = V_s I_s^* \text{-----(1)}$$

$$S_r = P_r + jQ_r = V_r I_r^* \text{-----(2)}$$

The active and reactive powers are found by using the Equations as below.

$$P_s \approx \frac{3}{2} \overline{(v_s)} i_{sy} = -\frac{3}{2} \overline{(v_s)} \frac{L_m}{L_s} i_{ry} \text{-----(3)}$$

$$Q_s \approx \frac{3}{2} \overline{(v_s)} i_{s\alpha} = -\frac{3}{2} \overline{(v_s)} \frac{L_m}{L_s} (|i_{ms} - i_{rx}|) \\ \approx \frac{3}{2} \overline{(v_s)} \frac{L_m}{L_s} (\frac{|v_s|}{2\sqrt{3}L_m} - i_{rx}) \text{-----(4)}$$

4. Dynamic behavior of DFIG in the rotor reference frame

The equivalent circuit of the DFIG in the rotor reference frame rotating at the rotor speed is shown in Figure 2. The rotor reference frame is represented as αr and βr .

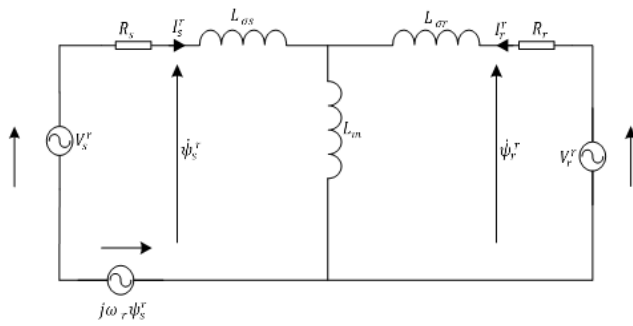


Fig. 5. Equivalent circuit of DFIG in rotor reference frame ($\alpha_r - \beta_r$)

The rotor flux linkage vectors can be expressed as

$$\begin{aligned} \psi_s^r &= L_s I_s^r + L_m I_r^r \\ \psi_r^r &= L_m I_r^r + L_m I_s^r \end{aligned} \quad (5)$$

According to the rotor flux linkages the stator current can be calculated as

$$I_s^r = \frac{L_r \psi_s^r - L_m \psi_r^r}{L_s L_r - L_m^2} = \frac{\psi_s^r}{\sigma L_s} - \frac{L_m \psi_r^r}{\sigma L_s L_r} \quad (6)$$

where $\sigma = \frac{(L_s L_r - L_m^2)}{L_s L_r}$ is the leakage factor. From the equivalent circuit of DFIG, stator voltage vectors can be expressed as

$$V_s^r = R_s I_s^r + \dot{\psi}_s^r + j\omega_r \psi_s^r \quad (7)$$

From the stator voltage and current the stator active power input from the grid can be expressed as

$$P_s = \frac{3}{2} V_s^r \cdot I_s^r = \frac{3}{2} (R_s I_s^r + \dot{\psi}_s^r + j\omega_r \psi_s^r) \cdot I_s^r \quad (8)$$

Neglecting the stator copper loss, the above equation becomes

$$P_s = \frac{3}{2} (\dot{\psi}_s^r + j\omega_r \psi_s^r) \cdot I_s^r \quad (9)$$

In the same way the reactive power output to the grid is expressed as

$$Q_s = -\frac{3}{2} V_s^r * I_s^r = -\frac{3}{2} (\dot{\psi}_s^r + j\omega_r \psi_s^r) * I_s^r \quad (10)$$

The relationship between the stator and rotor flux in the stationary α - β and rotor α_r - β_r reference frame is shown in Figure 3

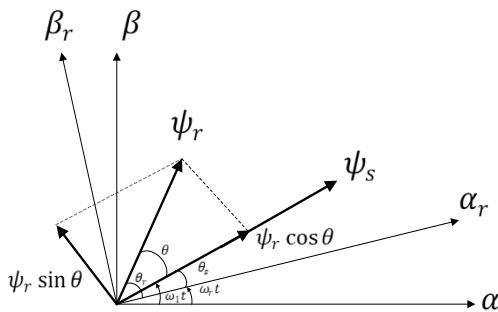


Fig. 6. Relation of stator and rotor flux linkage vectors in stationary and rotor reference frames

The stator and rotor fluxes in rotor reference frame is given

by,

$$\psi_s^r = |\psi_s^r| \cdot e^{j\theta_s} \quad (11)$$

$$\psi_r^r = |\psi_r^r| \cdot e^{j\theta_r} \quad (12)$$

The transformation of stator flux on the reference frame is given by

$$\psi_s^r = \psi_s^s \cdot e^{-j\omega_r t} \quad (13)$$

The relationship between stator and rotor flux is given by

$$\dot{\theta}_s = \omega_1 - \omega_r \quad (14)$$

The stator flux on the stationary reference is given by

$$\psi_s^s = \int (V_s^s - R_s I_s^s) dt \quad (15)$$

Assuming that the stator is connected to the balanced ac network such that and there is no change in rotor speed for the analysis. Normally due to the large inertia of the wind turbine the rotor speed will not change. The stator flux on the rotor reference frame is given by

$$|\psi_s^r| = |\psi_s^s e^{-j\omega_r t}| = |\int V_s^s dt| = \text{constant} \quad (16)$$

$$\frac{d|\psi_s^r|}{dt} = 0 \quad (17)$$

$$\dot{\psi}_s^r = |\psi_s^r| j \dot{\theta}_s e^{j\theta_s} = j(\omega_1 - \omega_r) \psi_s^r$$

Based on the equations (6), (9), (13) and (18) the stator active power input and reactive power output is given by

$$P_s = -\frac{3}{2} \frac{L_m}{\sigma L_s} \omega_1 |\psi_s^r| |\psi_r^r| \sin \theta \quad (18)$$

$$Q_s = \frac{3}{2} \frac{L_m}{\sigma L_s} |\psi_s^r| \left(\frac{L_m}{L_r} |\psi_r^r| \cos \theta - |\psi_s^r| \right) \quad (19)$$

Where $\theta = \theta_r - \theta_s$ is the angle between the stator and rotor flux linkage vectors.

Differentiating (18) and (19) results in the following equations

$$\frac{dP_s}{dt} = -\frac{3}{2} \frac{L_m}{\sigma L_s L_r} \omega_1 |\psi_s^r| \frac{d(|\psi_r^r| \sin \theta)}{dt} \quad (20)$$

$$\frac{dQ_s}{dt} = \frac{3}{2} \frac{L_m}{\sigma L_s L_r} \omega_1 |\psi_s^r| \frac{d(|\psi_r^r| \cos \theta)}{dt} \quad (21)$$

From equations (20) and (21) it is found that the active and reactive power depends on $|\psi_r^r| \sin \theta$ and $|\psi_r^r| \cos \theta$ respectively. The $|\psi_r^r| \sin \theta$ and $|\psi_r^r| \cos \theta$ are the perpendicular components of the rotor flux in the direction of stator flux. This indicates that the change in the rotor flux will change the active (P_s) and reactive powers (Q_s). It is also found that the initial status of the rotor position will not affect the active (P_s) and reactive powers (Q_s).

5. Simulation results

The doubly fed induction generator based power generation system is simulated in MATLAB software. A 5 MW DFIG is considered for the simulation studies. The two converters, one for grid side and another for rotor side are developed in simulation model. In the grid side AC to DC converter is used to convert grid ac voltage into dc and maintains dc voltage in the dc link. The dc link voltage is 1000V. Since the converter produce harmonics a RC filter is connected. The capacitor value

of the RC filter is $200\mu\text{F}$. This RC filter will absorb the switching harmonics of the converter. The rotor side converter is DC to AC inverter, which is used to control the active and reactive power from the proposed direct power control strategy. The purpose of the grid side converter is to maintain the dc link voltage to a constant value of 1000V. The switching frequency of the converter is 2kHz and the series reactor is 0.3mH.

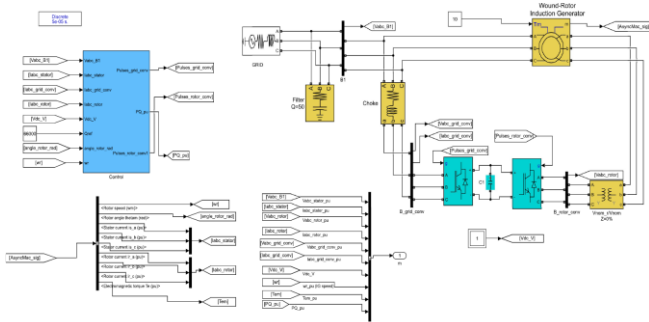


Fig. 7. Simulation model of DFIG by the proposed direct power control

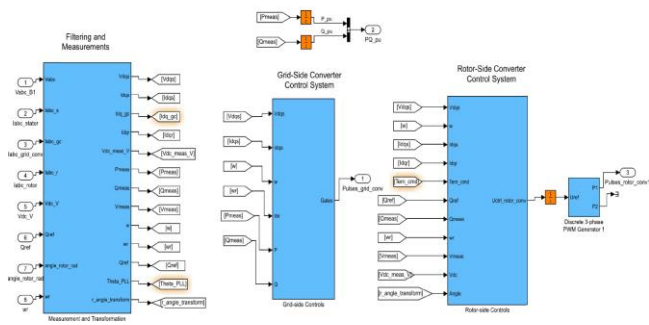


Fig. 8. Direct Power Control Scheme

First the grid side converter is operated to regulate the dc link voltage. Then the stator of the DFIG is excited. The rotor speed is set externally. After 0.2 Sec rotor side converter is enabled. The initial stator real and reactive power being set as -2.5MW and -0.7Mvar respectively. The negative sign indicates that the real power is generated and the reactive power is absorbed. The real and reactive power is varied by the proposed direct power control with constant rotor speed.

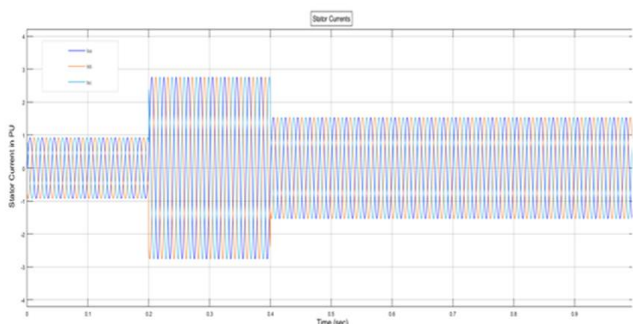


Fig. 9. Simulation results of step change of active and reactive power with constant rotor speed

For the step change of active and reactive power there is overshoot of either the stator or rotor currents. Simulation is carried for other step change of active and reactive power with constant rotor speed. For any variations of active and reactive step change or any other fixed rotor speed there is no stator or rotor current overshoot. This shows the effectiveness of the proposed direct power control for the doubly fed induction generator.

6. Conclusion

This paper presents a DFIG wind turbine control study using a direct power control design. which compares the proposed control scheme with the conventional standard DFIG control method. it shows that under the direct-current vector control configuration, how the integrated GSC and RSC control is designed to implement the dc-link voltage, real power, reactive power, and grid voltage support control functions. Comprehensive simulation studies demonstrate that the proposed DFIG wind turbine control structure can effectively accomplish wind turbine control objectives with superior performance under both steady and variable wind conditions within physical constraints of a DFIG system. Beyond physical constraints of a DFIG system, the proposed control approach operates the system by regulating the RSC for real and reactive power control and by controlling the GSC to stabilize the dc-link voltage as the main concern. The direct-current vector current structure is also effective for peak power tracking, power factor improvement and grid voltage support control under a low voltage sag condition.

References

- [1] S. Li, T. A. Haskew, K. A. Williams and R. P. Swatloski, "Control of DFIG Wind Turbine with Direct-Current Vector Control Configuration," in *IEEE Transactions on Sustainable Energy*, vol. 3, no. 1, pp. 1-11, Jan. 2012.
- [2] Shuhui Li, Timothy A. Haskew, Yang-Ki Hong and Ling Xu, "Direct-current vector control of three-phase grid-connected rectifier-inverter," in *Electric Power Systems Research*, vol. 81 pp. 357-366, 2011.
- [3] Ahmed G and Abo-Khalil, "Synchronization of DFIG output voltage to utility grid in wind power system" *Renewable Energy*, vol. 44 pp. 193-198, 2012.
- [4] D. Zhi and L. Xu, "Direct Power Control of DFIG with Constant Switching Frequency and Improved Transient Performance," in *IEEE Transactions on Energy Conversion*, vol. 22, no. 1, pp. 110-118, March 2007.
- [5] Gaillard A. P. Poure and S. Saadate, "Variable speed DFIG wind energy system for power generation and harmonic current mitigation," *Renewable Energy*, vol. 34, pp. 1545-1553, 2009.
- [6] E. Heydari and A. Y. Varjani, "Combined modified P&O algorithm with improved direct power control method applied to single-stage three-phase grid-connected PV system," *2018 9th Annual Power Electronics, Drives Systems and Technologies Conference (PEDSTC)*, Tehran, 2018, pp. 347-351.
- [7] Gayathri Nair S and N. Senroy, "Comparative analysis of storage systems in a microgrid with MTDC based DFIG connection," *2016 IEEE Region 10 Conference (TENCON)*, Singapore, 2016, pp. 627-631.
- [8] Khatun, Mst. Farzana and Md. Rafiqul Islam Sheikh, "Low voltage ride through capability enhancement of DFIG-based wind turbine by a new topology of fault current limiter," *2016 2nd International Conference on Electrical, Computer & Telecommunication Engineering (ICECTE)*, pp. 1-5, 2016.

- [9] Y. Jiao, H. Nian and G. He, "Control strategy based on virtual synchronous generator of DFIG-based wind turbine under unbalanced grid voltage," *2017 20th International Conference on Electrical Machines and Systems (ICEMS)*, Sydney, NSW, 2017, pp. 1-6.
- [10] B. G. Teshager, H. Minxiao, S. Patrobers, Z. W. Khan, L. K. Tuan and F. M. Shah, "Direct power control strategy based variable speed pumped storage system for the reduction of the wind power fluctuation impact on the grid stability," *2018 IEEE 12th International Conference on Compatibility, Power Electronics and Power Engineering (CPE-POWERENG 2018)*, Doha, 2018, pp. 1-6.
- [11] T. Wang, Y. Xiao, X. Zhang and D. Xu, "Impedance-based stability analysis of DFIG," *2016 IEEE Energy Conversion Congress and Exposition (ECCE)*, Milwaukee, WI, 2016, pp. 1-4.
- [12] Yunfei Wang, Xing Zhang, Zhen Xie and Hui Yang, "Model predictive direct current control of DFIG at low switching frequency," *2016 IEEE 8th International Power Electronics and Motion Control Conference (IPEMC-ECCE Asia)*, Hefei, 2016, pp. 1432-1435.
- [13] D. Jiandong, S. Lei, C. Shuaishuai, H. Yu and L. Wuji, "Research on adaptive current instantaneous trip protection for active distribution network line with DFIGs," *2016 China International Conference on Electricity Distribution (CICED)*, Xi'an, 2016, pp. 1-5.
- [14] S. Swain and P. K. Ray, "Ride-through capability improvement of a grid-integrated DFIG based wind turbine system using a new protection design," *2016 IEEE 6th International Conference on Power Systems (ICPS)*, New Delhi, 2016, pp. 1-5.
- [15] X. Zhu and Z. Pan, "Study on the influencing factors and mechanism of SSR due to DFIG-based wind turbines to a series compensated transmission system," *2017 IEEE 26th International Symposium on Industrial Electronics (ISIE)*, Edinburgh, 2017, pp. 1029-1034.